

AN RF SEPARATOR FOR CLOUD MUONS AT TRIUMF

J.A. Macdonald, E.W. Blackmore, D.A. Bryman, J. Doornbos, K.L. Erdman  
R.M. Pearce, R.L. Poirier, J.-M. Foutissou and J. Spuller  
TRIUMF, 4004 Westbrook Mall, Vancouver, B.C., Canada V6T 2A3

Summary

A particle separator utilizing a magnetic field crossed with an rf electric field has been built and incorporated into the M9 secondary channel to produce a clean negative muon beam at 77 MeV/c  $\pm$  5%. The separator is driven at the main cyclotron frequency (23 MHz) and phase locked to the primary proton beam. Separation is achieved by using both the temporal and velocity differences between the muons, produced near the production target (cloud muons), and both the pion and electron contaminants in the beam.

Introduction

In early beam studies of the M9 stopped pion channel<sup>1</sup> it was recognized that the intensity of muons in pion beams of ~60-120 MeV/c was sufficient to be useful for a number of muon experiments being considered at TRIUMF. These so-called cloud muons are typically about 10% of the pion flux after 8-10 m drift and are produced in pion decay in flight near the production target. They have a well-defined time structure (determined by the cyclotron rf) and momentum bite (determined by the channel acceptance). Moreover they come from a relatively well-defined source near the production target and therefore behave well optically in the channel and can be focused to a good beam spot of high luminosity. For some experiments, however, the pion and electron contamination in the beam contributes an unacceptable background due to pion decay or capture near the experimental target or causes serious rate problems in detectors; some form of particle separation in the channel is then required.

The motivation to develop a clean muon beam was enhanced when the experimental program to study exotic decay modes of the muon in a time projection chamber (TPC) was proposed.<sup>2</sup> The experiment and detector were well matched to the potential  $\mu^-$  stopping rate from M9 of the order of  $10^6$  s<sup>-1</sup> but required pion contamination of  $<10^{-2}$ . The time structure of the beam in the momentum range of immediate interest (70-80 MeV/c) suggested separation by an rf field at the cyclotron frequency was possible.

Beam Optics

The layout of the complete beam line is shown in Fig. 1. The original M9 beam line terminated at the focus F2; the extension was designed to retain this short version

and to include two experimental locations after the separator: W3, a general location for several experiments and W4, a fixed location for the TPC facility. The cloud muons originate from the decay of pions in flight in the vicinity of the production target IAT2 in the proton beam line BL1A. The vertical source size (determined by the phase space acceptance) seen by the channel at F2 is about 2.5 cm.

The principle of operation can be seen in Fig. 2 which shows the time-of-flight structure of the secondary beam at the location of the middle of the separator (12.1 m from IAT2) for a 77 MeV/c ( $\pm$ 5%) beam. The muons ( $\beta=0.6$ ) arrive approximately one-half an rf period separated from the pions ( $\beta=0.5$ ) from the same 5 ns wide proton pulse and electrons ( $\beta=1.0$ ) from the following proton pulse. The phase of the separator is adjusted so that the peak of the rf voltage coincides approximately with the muons; the force of the electric field is exactly compensated by the  $\vec{v} \times \vec{B}$  force of a horizontal dc

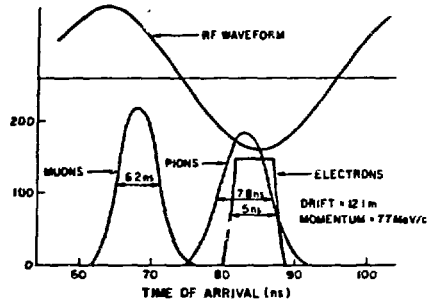


Fig. 2. Time structure of beam in the separator relative to the rf on the electrodes.

magnetic field. Ideally, pions and electrons arrive 180° later when the electric field is reversed. Then electric and magnetic forces work in the same direction to deflect these particles.

Consider first the case of dc electric and magnetic fields. Then we have for the deflection of muons,

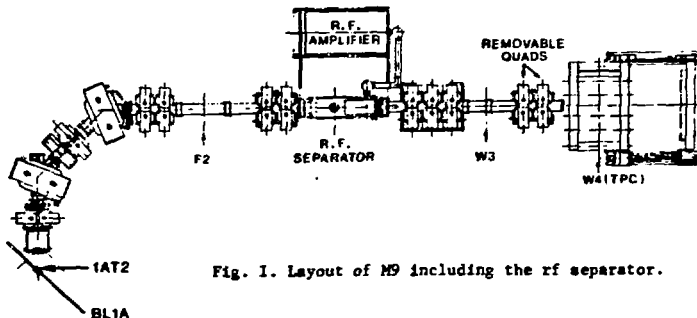


Fig. 1. Layout of M9 including the rf separator.

$$y'_\mu = \frac{z}{10^6 \times P} \left( 300 B - \frac{E}{\beta_\mu} \right),$$

where  $y'_\mu$  is the angular deflection for muons in radians  $z$  is the length of separator in centimetres,  $B$  the magnetic field in kilogauss,  $E$  the electric gradient in kilovolt/centimetre, and  $P$  the momentum in  $\text{GeV}/c$ .  $B$  and  $E$  are chosen so that  $y'_\mu=0$  and therefore  $300 B = E/\beta_\mu$ . But in the case of the rf separator, the electric field has changed sign for the  $\nu$ 's and  $e$ 's so that then for the other particles,  $p$

$$y'_p = \frac{z}{10^6 \times P} \left( 300 B + \frac{E}{\beta_p} \right) = \frac{z \cdot E}{10^6 \times P} \left( \frac{1}{\beta_\mu} + \frac{1}{\beta_p} \right).$$

Beam calculations were carried out using the programs TRANSPORT and REVMOG. The plate length and gap constraints were first determined from the beam optics. In addition the plate length is limited by the transit time (3.3 ns/m for electrons, 5.6 ns/m for muons and 6.8 ns/m for pions) which can add to excessive dispersion through the separator. From this and considering the power limitations of the available transmitter, plate dimensions were chosen. The deflections obtainable for  $\nu$ 's and  $e$ 's with these values are  $y'_\nu = 123 \text{ mrad}$  and  $y'_e = 87 \text{ mrad}$ , respectively. Using these parameters the beam line as a whole was then optimized leading to the positioning and current settings of quadrupole elements in the extension.

In practice it is not possible to have a  $180^\circ$  phase difference between  $\mu$  and  $\nu$  and simultaneously between  $\mu$  and  $e$ . At the centre of the separator both  $\nu$  and  $e$  are  $120^\circ$  out of phase with the  $\mu$ 's. The phase of the rf wave shown in Fig. 2 is taken in such a way to maximize muon flux and at the same time minimize the pion contamination. The effect of phase tuning of the separator on the overall muon transmission to the final focus and on the pion and electron contamination is shown in Fig. 3.

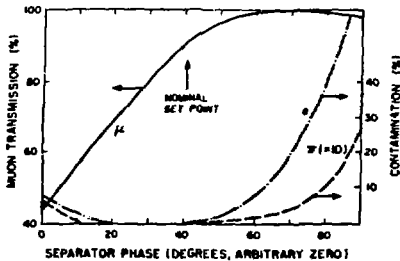


Fig. 3. Effect of separator phase on beam composition: left scale muon transmission and right scale  $\nu$  and  $e$  contamination.

A typical example of the separating effect of the separator from REVMOG is given in Fig. 4 for a peak electric field gradient of  $17 \text{ kV/cm}$  and a magnetic field of  $80 \text{ G}$ . Figure 4(a) gives the resulting distributions of the vertical position,  $y$ ,  $1.5 \text{ m}$  from the exit of the separator near the entrance of the following quadrupole. Figure 4(b) gives the distributions for the vertical angle  $y'$ . In both cases a long pion tail overlaps the muon distribution. We have included vertical slits at this location in the final design to allow the option of refining the pion and electron separation at the expense of 10% to 20% of the muon flux.

The criteria of momentum acceptance ( $\sim 10\% \Delta P/P$ ), muon flux ( $\sim 10^6/\text{s}$ ) and beam spot at the TPC target ( $8 \times 8 \text{ cm}^2$ ) were shown by the beam calculations to be feasible.

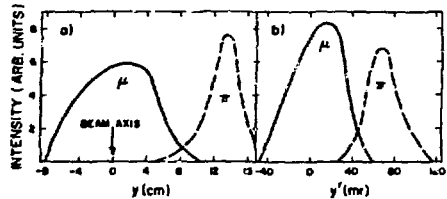


Fig. 4. Calculated separation of  $\pi$ 's from  $\mu$ 's after the separator a) vertical position  $y$ , b) vertical angle  $y'$ .

### RF System

The rf power for the separator is supplied by a modified  $120 \text{ kW}$  rf amplifier that was initially used for the central region cyclotron model work. It is a standard class "C" amplifier using an Eimac 4CW 250000A tetrode. The standing wave section of transmission line which transfers the power to the resonator coupling loop is terminated at each end with a variable vacuum capacitor to provide a  $\pi$  network matching section. The coupling loop is water cooled and the ceramic feedthrough is a coaxial structure similar to the coupling loop used in the TRIUMF  $500 \text{ MeV}$  cyclotron.

The design of the resonators for the separator was constrained by the available physical space, determined by the existing beam line height and its components, and the physical size of the electrodes (plates) determined by the beam line optics calculations. The peak plate-to-plate voltage required was  $>300 \text{ kV}$ . The two resonator assemblies operate in push-pull mode each at  $\pm 160 \text{ kV}$  to ground. The height of the beam line made it necessary to have a  $90^\circ$  bend in the lower resonator structure; the upper resonator was built to be identical for symmetry and compactness. The electrodes also had to be specially shaped in order to provide a uniform field distribution across the width of the plates. A structure separate from the vacuum box was constructed out of copper to provide an rf liner which completely encloses the electrodes except for the apertures at both ends to allow the beam to pass through. The rf structure design parameters are shown in Table I.

Table I  
TRIUMF rf Separator Parameters

Electrodes	width	25 cm	
	length	100 cm	
	gap	15 cm	
	gradient	21 kV/cm	
	voltage	$\pm 160 \text{ kV/cm}$	
RF liner	width	45 cm	
	length	115 cm	
	height	38 cm	
Vacuum chamber	width	58.4 cm	
	length	123.8 cm	
	height	51.4 cm	
	typical pressure	$5 \times 10^{-7} \text{ Torr}$	
Resonators	Tip	Root	
	i.d.	7.6 cm	7.6 cm
	o.d.	17.8 cm	40.6 cm
	$Z_0$	50 $\Omega$	100 $\Omega$
	length	60 cm	99 cm
	frequency	23.06 MHz	
	power	100 kW	
	Q	5000	
magnetic field coil	0.41 gauss/amp @ 100 gauss		

The 72 pfd of electrode capacity, determined by their size and the beam gap, has a foreshortening effect of  $62.5^\circ$  of electrical length. While this makes the structure shorter it also increases the power requirements and hence increases the current density especially at the inner conductor. Typical current densities are 88 A/cm on the surface of the inner conductor at the shorted end of the 100  $\Omega$  section of line and 55 A/cm on the surface of the vertical stem and the electrodes. Because of these high current densities good electrical contact becomes very important. All the rf surfaces are water cooled.

A drawing of the rf separator is shown in Fig. 5. The electrodes are cantilevered and supported only at the root of the 100  $\Omega$  section of line and at the extended end of the inner conductor. The coarse tuning is done via vacuum feedthrough adjusting screws which adjust the rf liner walls in and out. The fine tuning is accomplished by adjusting the extended end of the inner conductor. This has a combined effect of changing the electrode capacity and the characteristic impedance of the line sections for frequency adjustments.

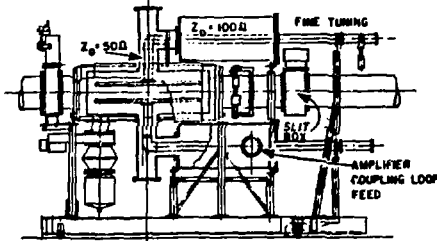


Fig. 5. Line drawing of the rf separator (side view). Beam enters from the left.

### RF Tests

The problems encountered were mainly those dealing with high power operation, the first one being the production of several hundred mr/h of X-rays which necessitated the building of shielding walls making the resonator inaccessible during tests. Our first major problem was the failure of finger-stock in the vertical section of the resonator. This was replaced by a clamped knife edge ring. Once the separator was installed in the beam line the major downtime was due to the damage of the beam line vacuum windows from rf leakage. This problem was solved by shielding the windows completely from the electrodes by reducing the beam aperture in the rf liner. The window material was changed from 6.4  $\mu$ m Al-mylar to 19  $\mu$ m Al metal.

In order to determine the plate voltage one of the voltage probes was calibrated directly at low power. This gave about a 20% measurement which was compatible with estimates from the power developed and Q. The best confirmation of plate voltage was obtained from the muon beam performance and the optimized value of the crossed magnetic field.

The major operational difficulty with the separator has been a phase instability between the coupling loop and the electrode. When the amplifier-resonator system is optimally tuned, this instability is of the order of  $\pm 10^\circ$  maximum and  $25^\circ$  typical. As can be seen from Fig. 3 this leads to some loss of transmission and poorer separation of pions and electrons.

### Beam Tests

The channel was first tuned to obtain maximum transmission with the separator turned off. The optimized values for most magnetic elements was within 10% of the calculated values. The separator was then powered up to nominal values of the rf power and crossed magnetic field calculated from the beam studies for 77 MeV/c muons. These values proved to be close to the optimum for transmission of muons and good pion and electron rejection.

The separator was driven from a signal picked up from the main cyclotron resonator. This signal was phase locked to a second signal obtained from a capacitive probe in the proton beam line; this eliminated any phase uncertainty due to the tuning of the cyclotron. The phase of the separator relative to the muon beam is determined by a variable delay in the capacitive probe signal fed to the phase-locking circuit.

The profile of the beam was measured with a 14-element hodoscope at the target position in the TPC. Figure 6 shows profiles taken with this device in both x (horizontal) and y (vertical) planes. The beam must pass through a 20 cm diameter hole in the front of the TPC magnet; the profiles in Fig. 6 correspond to about 80% of the muon beam incident at the entrance of the TPC magnet, or about  $8 \times 10^5 \mu^- s^{-1}$  for 100  $\mu$ A of protons on a 10 cm Be production target at 1A2T.

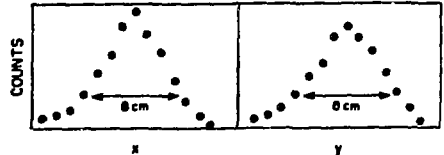


Fig. 6. Beam profiles for muons measured at the TPC target position. x: horizontal, y: vertical.

The pion contamination of the beam at the entrance of the TPC magnet was determined from the time-of-flight spectrum of the beam to be about 0.1%; electrons are about 1%.

The pion contamination in beam reaching the TPC target is further reduced by degrading and collimators. The pion contamination here was determined from analysis of events in the TPC itself by observing the number of high energy protons following  $\pi^+$  absorption. The pion contamination in the incident beam was determined to be  $< 2 \times 10^{-4}$ .

### Acknowledgement

We are pleased to acknowledge the assistance at various points in the design and execution of the rf separator of R. Burge, J. Cresswell, D. Evans, J. Love, C. Mannes, J. McIlroy, A. Otter, P. Schmor, R. Sprenger, R. Trelic, G. Waters and J. Yandou.

### References

1. H.M.H. Al-Qazzaz et al., The TRIUMF stopped  $\pi$ - $\mu$  channel, Nucl. Instrum. Meth. 16, 35 (1980).
2. C.K. Hargrove et al., Proc. Int. Conf. Instrumentation for Collider Beam Physics SLAC-250, p.41 (1982).